(b) With 7-Hydroxyhept-2-enoic Acid (17, G = CO_2H). The acid[33] underwent no ^1H NMR spectroscopic change (except at OH) on being kept at 100 °C with 0.5 M NaOD-D_2O for 6 h.

(c) With Methyl 7-hydroxyhept-2-enoate (17, G = CO_2Me). The ester was kept with an excess of 0.5 molar aqueous sodium hydroxide at 20 °C for 6 h. Acidification and extraction gave tetrahydropyranylacetic acid (97%).

Acknowledgment. We thank S.R.C. for provision of equipment and a maintenance grant (to R.J.P.).

Ground- and Excited-State Oxidation-Reduction Chemistry of (Triphenyltin)- and (Triphenylgermanium)tricarbonyl(1,10-phenanthroline)-rhenium and Related Compounds

John C. Luong, Robert A. Faltynek, and Mark S. Wrighton*

Contribution from the Department of Chemistry, Massachusetts Institute of Technology, Cambridge, Massachusetts 02139. *Received May 16, 1980*

Abstract: Optical absorption and emission spectroscopy and the photochemistry and electrochemistry are reported for complexes of the general formula $R_3EM(CO)_3L$ (R = Ph or Me; E = Ge or Sn; M = Mn or Re; L = 1,10-phenanthroline, 2,2′-bipyridine, or 2,2′-biquinoline). The lowest excited state in each system results from charge-transfer, $(E-M)\sigma_b \rightarrow \pi^*L$, absorption. Several of the Re complexes (R = Ph; E = Ge or Sn; L = 2,2′-bipyridine or 1,10-phenanthroline) exhibit optical emission from the lowest excited state at 298 K in fluid solution; emission lifetimes under such conditions for these complexes are $\sim 10^{-6}$ s. These excited complexes can be quenched by both electron-donor quenchers and by electron-acceptor quenchers. Detailed quenching studies of $Ph_3SnRe(CO)_3(phen)$ (phen = 1,10-phenanthroline) have been carried out, and quenching obeys Stern-Volmer kinetics. Electron donors, Q, for which $E°(Q^+/Q)$ is more negative than $\sim +0.2$ V vs. SCE quench at an essentially diffusion-controlled rate. Electron acceptors, P^+, for which $E°(P^+/P)$ is more positive than ~ -1.0 V vs. SCE also quench at nearly a diffusion-controlled rate. Cyclic voltammetry of the complexes in CH_3CN/0.1 M $[n\text{-}Bu_4N]ClO_4$ typically shows a one-electron, reversible reduction in the −1.1 to −1.7 V vs. SCE range associated with the population of the lowest available π^* orbital principally localized on L. An irreversible oxidation current peak is observed in the range +0.5 to +0.8 V vs. SCE. The M-containing oxidation product is *fac*-$[(CH_3CN)M(CO)_3L]^+$. Consistent with the ground state electrochemistry, quenching by reversible electron-donor quenchers (e.g., *N,N,N′,N′*-tetramethyl-*p*-phenylenediamine) results in no net photoredox reaction ($\Phi < 10^{-3}$) whereas quenching by reversible electron-acceptor quenchers (e.g., *N,N′*-dimethyl-4,4′-bipyridinium) results in net redox chemistry to reduce the quencher and to form *fac*-$[(CH_3CN)M(CO)_3L]^+$ from the complex. The data are consistent with primary formation of $R_3E\cdot$ and the 16-valence electron $[M(CO)_3L]^+$ from cleavage of the $[R_3EM(CO)_3L]^{+\cdot}$ formed by excited-state electron transfer. Rate of $[R_3EM(CO)_3L]^{+\cdot}$ cleavage is similar to the dissociative E-M bond cleavage induced by the $(E-M)\sigma_b \rightarrow \pi^*L$ optical excitation.

A molecule in its lowest one-electron excited state should have reactivity properties related to the ground state of the one-electron oxidized molecule and the ground state of the one-electron reduced molecule. This statement follows from the simple orbital diagrams in Scheme I for a metal complex having a lowest metal to ligand charge-transfer excited state. The excited species has a "hole" in the lowest orbital like the one-electron oxidized molecule, and simultaneously the excited species has an electron in the highest orbital like the one-electron reduced molecule. Though such schemes are an oversimplification of the situation, such a view of excited-state reactivity leads to some fairly straightforward expectations. Such schemes should have particular value for many inorganic and organometallic molecules where the HOMO and LUMO of the molecule often play a very different role in the bonding.[1]

As an example of the value of such one-electron considerations in inorganic systems consider the six-coordinate, low-spin d^6 complexes that have been studied with respect to photosubstitution.[1,2] In all of these systems that are photosubstitution labile the HOMO is a π d orbital that is either nonbonding or weakly π bonding. By way of contrast, the LUMO is a σ d orbital that

Scheme I. One-Electron Orbital Diagrams for a Metal Complex, M-L, in Its Ground State, and in Its MLCT Excited State, Reduced by One Electron and Oxidized by One Electron

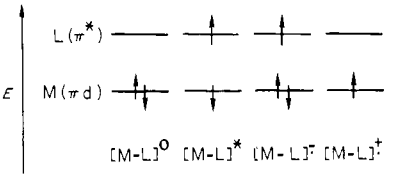

is strongly antibonding with respect to the metal-ligand bond. The lowest one-electron excited state then involves population of an orbital which is strongly σ antibonding, resulting in a very labile excited species. The "hole" generated in the π d level is not too consequential with respect to lability. These excited-state expectations are consistent with the existence, and indeed isolability, of various pairs of d^5/d^6 systems, e.g., $Fe(CN)_6^{3-/4-}$, $V(CO)_6^{0/-}$, and $Ru(NH_3)_6^{3+/2+}$, whereas attempted addition of an electron to the simple low-spin d^6 systems does not seem to result in an isolable d^7, six-coordinate complex. Presumably, the lowest orbital available in the low-spin d^6 system is a strongly σ-antibonding level whose occupation results in loss of a ligand; e.g., $Co(CN)_6^{3-} \xrightarrow{+e^-} Co(CN)_5^{3-} + CN^-$.

In this article we wish to report the results of a study of the ground-state electrochemistry and excited-state electron transfer of the organometallic complexes $Ph_3ERe(CO)_3(phen)$ (E = Sn, Ge; phen = 1,10-phenanthroline) and related species. The results

(1) Geoffroy, G. L.; Wrighton, M. S. "Organometallic Photochemistry"; Academic Press: New York, 1979.

(2) (a) Balzani, V.; Carassiti, V. "Photochemistry of Coordination Compounds"; Academic Press: New York 1970. (b) "Concepts of Inorganic Photochemistry"; Adamson, A. W., Fleischauer, P. D., Eds.; Wiley: New York, 1975. (c) Ford, P. C. *Rev. Chem. Intermed.* **1979**, *2*, 267.

0002-7863/80/1502-7892$01.00/0

Table I. Solvent Dependence on MLCT band max, nm, M → LCT $R_3ERe(CO)_3L$ at 298 K

complex	solvent	band max, nm M → LCT
$Ph_3SnRe(CO)_3(phen)$	CH_3CN	430, 325 sh
	THF	460, 330 sh
	CH_2Cl_2	465, 330 sh
	EPA	470, 330 sh
	benzene	478, 330 sh
	isooctane	510, 370 sh, 340
$Me_3SnRe(CO)_3(phen)$	CH_3CN	475, 330
	CH_2Cl_2	505, 340
	EPA	515, 340
	benzene	520, 345
	isooctane	565, 365
$Ph_3SnRe(CO)_3(biquin)$	CH_3CN	547
	THF	575
	CH_2Cl_2	560
	benzene	600

show that removal of an electron from the HOMO results in substantial lability whereas addition of an electron to the LUMO does not result in labilization, consistent with our preliminary findings[3] concerning the photochemistry of these complexes associated with an excited state involving (E–Re)$\sigma_b \rightarrow \pi^*$phen CT. With reference to Scheme I, these species feature lowest excited states involving increased electron density on the 1,10-phenanthroline and decreased electron density in the E–Re bond compared to the ground electronic state. Thus, the population of the LUMO localized on the ligand results in a species having greater reducing power than the ground state, and depopulation of the HOMO localized on the E–Re core results in enhanced oxidizing power of the excited compared to the ground state. Further, the excited species should have reactivity properties in common with the ground-state species $[Ph_3ERe(CO)_3(phen)]^{-\cdot}$ and $[Ph_3ERe(CO)_3(phen)]^{+\cdot}$.

Results and Discussion

(a) Synthesis of Complexes. The $R_3EM(CO)_3L$ (R = Ph, Me; E = Ge, Sn; M = Mn, Re; L = 2,2′-bipyridine (bpy), 1,10-phenanthroline (phen), 2,2′-biquinoline (biquin)) complexes prepared for study were synthesized generally according to the chemistry represented by eq 1–3.[3] For M = Mn, such compounds

$$M(CO)_5Cl \xrightarrow[\Delta]{L} ClM(CO)_3L + 2CO \quad (1)$$

$$ClM(CO)_3L \xrightarrow{Na/Hg} [M(CO)_3L]^- + Cl^- \quad (2)$$

$$[M(CO)_3L]^- + R_3EX \xrightarrow[\Delta]{} R_3EM(CO)_3L + X^- \quad (3)$$

have been made previously by reaction of L with $R_3EMn(CO)_5$.[4] The details of the synthesis and purification of representative complexes are given in the Experimental Section. The $R_3EM(CO)_5$ complexes are prepared according to the procedure represented by eq 4 and 5.[5] Complexes were characterized by IR,

$$M_2(CO)_{10} \xrightarrow{Na/Hg} 2[M(CO)_5]^- \quad (4)$$

$$R_3EX + [M(CO)_5]^- \rightarrow R_3EM(CO)_5 + X^- \quad (5)$$

^1H NMR, and UV–vis spectroscopy and by elemental analyses. All of the complexes are soluble in common organic solvents and are thermally inert. In photochemical studies none of the complexes showed any detectable thermal chemistry on the same time scale.

(b) Electronic Absorption Spectra. Complexes of the formula $R_3EM(CO)_3L$ exhibit a fairly intense, solvent- and temperature-sensitive, visible absorption band that is not observed in the spectrum of $R_3EM(CO)_5$. A comparison of the absorption spectra of $Ph_3SnRe(CO)_5$, $Ph_3SnRe(CO)_3(phen)$, and $Ph_3SnRe(CO)_3(biquin)$ is shown in Figure 1; the solvent dependence on the first band for $R_3SnRe(CO)_3L$ is shown in Table I, and absorption data for all of the relevant complexes are given in Table II. Upon cooling of EPA solutions of the complexes to 77 K the absorption sharpens and the maximum blue-shifts significantly.

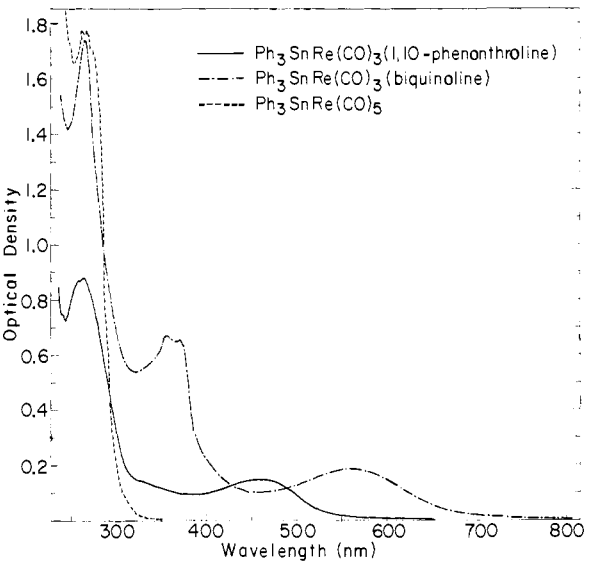

Figure 1. Electronic absorption spectra of representative $R_3EM(CO)_3L$ complexes in CH_2Cl_2 at 298 K. Extinction coefficients are given in Table II.

All of the optical absorption spectral data support the assignment of the lowest absorption in $R_3EM(CO)_3L$ as a CT band associated with (E–M)$\sigma_b \rightarrow \pi^*$L CT. The CT character and the direction of the CT are supported by the strong solvent effect and the dependence on L holding other variables constant. Many metal–carbonyl complexes are now known to exhibit solvent effects on absorption maxima such that more polar or polarizable solvents yield a blue-shifted maxima.[6] The red-shifted maximum for L = 2,2′-biquinoline vs. 2,2′-bipyridine or 1,10-phenanthroline is also commonly found for MLCT absorption.[6,7]

Three types of one-electron assignment for the lowest absorption can be specifically excluded by the optical data. Ligand field (d–d) transitions are ruled out, since such would be invariant in energy for a common coordination sphere in a situation like L = 2,2′-biquinoline vs. 2,2′-bipyridine. Ligand localized, intraligand (IL), excited states of L are not likely to be perturbed enough by coordination to yield any visible absorption. Finally, an (E–Re)$\sigma_b \rightarrow \sigma^*$ transition is ruled out on two counts: (i) $R_3EM(CO)_5$ shows no such visible absorption and (ii) such a transition, like other d–d transitions, would be insensitive to variation from L = 2,2′-bipyridine to L = 2,2′-biquinoline.

The infrared spectra in the CO stretching region for the various complexes have been measured and band maxima are given in Table III. The position of CO stretching frequencies in a homologous series of complexes is generally a good indication of relative charge density on the central metal. Interestingly, Me_3Sn– and $Ph_3SnRe(CO)_3(phen)$ exhibit a fairly significant difference in the position of their CO stretching frequencies. Paralleling the lower energy CO stretching frequency, that reflects greater electron density on Re, the $Me_3SnRe(CO)_3(phen)$ also exhibits a lower energy (E–Re)$\sigma_b \rightarrow \pi^*$L transition. Variations in CO stretching frequencies among the other complexes involving Sn–Re or Ge–Re bonds are modest.

Variation in the group bonded to the $M(CO)_3L$ moiety substantiates the conclusion that the orbital origin of the CT transition

(3) Luong, J. C.; Faltynek, R. A.; Wrighton, M. S. *J. Am. Chem. Soc.* **1979**, *101*, 1597.
(4) Ross, E. P.; Jernigan, R. T.; Dobson, G. R. *J. Inorg. Nucl. Chem.* **1971**, *33*, 3375.
(5) Jetz, W.; Simons, P. B.; Thompson, J. A. J.; Graham, W. A. G. *Inorg. Chem.* **1966**, *5*, 2217.
(6) (a) Wrighton, M. S.; Morse, D. L. *J. Organomet. Chem.* **1975**, *97*, 405. (b) Abrahamson, H. B.; Wrighton, M. S. *Inorg. Chem.* **1978**, *17*, 3385. (c) Giordano, P. J.; Wrighton, M. S. *Ibid.* **1977**, *16*, 160. (d) *J. Am. Chem. Soc.* **1979**, *101*, 2888.
(7) Wrighton, M.; Morse, D. L. *J. Am. Chem. Soc.* **1974**, *96*, 998.

Table II. Electronic Absorption Spectral Data

complex	solvent	λ_{max}, nm (ϵ, M^{-1} cm^{-1}) M → LCT	ligand-localized, π-π,* and others
$Ph_3SnRe(CO)_3(phen)$	CH_2Cl_2	465 (4600), 327 sh (4000)	265 (25 100)
$Ph_3SnRe(CO)_3(bpy)$	CH_2Cl_2	465 (4900), 347 (4300)	270 (21 300)
$Ph_3SnRe(CO)_3(biquin)$	CH_2Cl_2	570 (4000)	370 (21 400), 355 (20 400), 266 (51 600)
$Ph_3SnRe(CO)_5$	CH_2Cl_2	none	260 (14 600), 265 (14 600), 273 sh
$Me_3SnRe(CO)_3(phen)$	CH_2Cl_2	505 (5700), 340 (3900)	264 (25 500)
$Ph_3GeRe(CO)_3(phen)$	CH_2Cl_2	450 (5300), 330 (4000)	260 (35 000)
$Me_3SnRe(CO)_5$	heptane	none	260 (...)
$Ph_3SnMn(CO)_3(phen)$	CH_2Cl_2	504 (3000), 340 (5100)	266 (25 000)
$Ph_3SnMn(CO)_3(biquin)$	CH_2Cl_2	645 (3500), 415 (3900)	not measd
$Ph_3GeMn(CO)_3(phen)$	CH_2Cl_2	495 (5300), 333 (8000)	265 (29 000)
$Ph_3SnMn(CO)_5$	isooctane	none	270 sh (15 400), 265 sh (17 300), 266 sh (18 600), 255 sh (21 000)
$(OC)_5ReRe(CO)_3(phen)$	CH_2Cl_2	528 (7300), 350 sh (5200)	not measd
$ClRe(CO)_3(phen)$	CH_2Cl_2	380 (4000)	268 (30 600)
$BrMn(CO)_3(phen)$	CH_2Cl_2	420 (3150), 380 (3050)	320 (2070), 292 sh (17 300), 267 (34 500)
1,10-phenanthroline	CH_2Cl_2	NA	263 (33 100)
2,2'-bipyridine	CH_2Cl_2	NA	283 (14 500), 244 (10 000), 237 (11 000)
2,2'-biquinoline	CH_2Cl_2	NA	339 (18 800), 325 (23 100), 313 (20 100), 259 (66 000)
Ph_3SnCl	CH_2Cl_2	NA	269 (710), 264 (1060), 259 (1100), 253 (870)
Ph_3GeBr	CH_2Cl_2	NA	269 (1000), 264 (1340), 258 (1310), 253 (1080)
Me_3SnCl	isooctane	NA	no band max at $\lambda > 220$ nm

Table III. Infrared Spectral Data in the CO Stretching Region

complex	solvent	bands, cm^{-1} (ϵ, M^{-1} cm^{-1}, or abs ratio)
$Ph_3SnRe(CO)_3(phen)$	CH_2Cl_2	2004 (4700), 1903 (3840)
$Ph_3SnRe(CO)_3(bpy)$	CH_2Cl_2	2004 (3990), 1902 (3100)
$Ph_3SnRe(CO)_3(biquin)$	CH_2Cl_2	2002 (4200), 1903 (4020)
$Ph_3SnRe(CO)_5$	CH_2Cl_2	2114 (0.20), 2008 (1.0)
$Me_3SnRe(CO)_5$	CH_2Cl_2	2109 (0.18), 2000 (1.0)
$Me_3SnRe(CO)_3(phen)$	CH_2Cl_2	1989 (4760), 1890 (3800)
$Ph_3GeRe(CO)_3(phen)$	CH_2Cl_2	2004 (4870), 1900 (3730)
$Ph_3SnMn(CO)_3(phen)$	CH_2Cl_2	1986 (1.00), 1093 (0.57), 1888 (0.56)
$Ph_3SnMn(CO)_3(biquin)$	CH_2Cl_2	1979 (1.00), 1908 (0.70), 1890 sh (0.63)
$Ph_3GeMn(CO)_3(phen)$	CH_2Cl_2	1990 (4600), 1906 (2400), 1890 (2500)
$Ph_3SnMn(CO)_5$	isooctane	2094 (3330), 2027 (600), 2002 (13 900)
$(OC)_5ReRe(CO)_3(phen)$	CH_2Cl_2	2074 (0.33), 1992 (1.0), 1960 (0.85), 1886 (0.40)

is closely associated wiith the E–M σ bond. For the series $XRe(CO)_3(phen)$ (X = Cl, $Re(CO)_5$–, Ph_3Sn–), the energy of the first absorption maxima changes considerably. For the chloro complex the first maximum is at ~380 nm and is associated with a π d → π*L CT transition;[7] the (Cl–Re)σ_b level is presumably very stable. For X = Ph_3Sn– or $(OC)_5Re$–[8] the σ_b level is likely in the same vicinity as the π d level and photoelectron spectroscopy provides supporting data. For example, the binding energy of the electrons in the Mn–Cl σ bond in $Mn(CO)_5Cl$ is 11.08 eV whereas the binding energy for the electrons in the Mn–Sn σ bond in $Me_3SnMn(CO)_5$ is in the 8.63–9.01-eV region.[9] Further, ionization of the electrons in the Mn–Mn σ bond of $Mn_2(CO)_{10}$ requires only 8.02 eV. The binding energy of electrons in the Re–Cl σ bond of $Re(CO)_5Cl$ is 11.23 eV whereas the binding energy for the electrons in the Re–Re σ bond is 8.07 eV.[9,10] The binding energy of the π d electrons is also lowered in those cases where the σ electrons are more easily ionized, but the most easily ionized electrons in Re–Re bonded systems or Mn–Mn bonded systems would appear to be the σ electrons. In the Sn–M bonded systems the situation is less clear, but the absorption properties of $R_3EM(CO)_3L$ and $(OC)_5MM(CO)_3L$[8] are sufficiently similar that a common spectral assignment is reasonable. Thus, we conclude that the orbital diagram in Scheme II adequately represents the situation for the $R_3EM(CO)_3L$. Electrochemistry and photochemistry (vide infra) are consistent with the conclusion that the HOMO is the σ_b level and that the π*L level is the LUMO.

Scheme II. One-Electron Diagram for a Representative $R_3EM(CO)_3L$ Complex

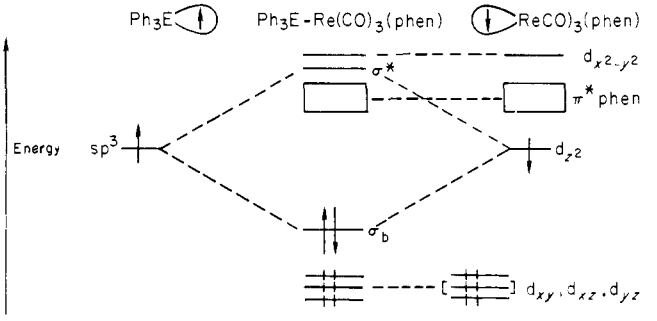

One other optical spectral feature of the complexes that can be assigned is the IL, π–π*, absorption associated with the 2,2'-bipyridine, 1,10-phenanthroline, or 2,2'-biquinoline (see Table II). Coordination of these ligands results in modest perturbation of the π–π* absorption feature of the uncomplexed ligands for L = bpy and phen. The lack of significant perturbation is consistent with the fact that the ligation principally involves binding via the N lone pairs.[11] For L = biquin we find that the IL absorption is red-shifted by an amount similar to that found upon protonating biquin by using HCl in EtOH.

The (E–M)σ_b → σ* transition in the $R_3EM(CO)_3L$ complexes is apparently too high in energy to be a prominent feature in the optical absorption, on the basis of properties of $R_3EM(CO)_5$. Ligand field transitions for the $EM(CO)_3L$ core are also likely obscured by other, more intense, absorption in the region.[6d,7]

(c) Luminescence Spectroscopy. Except for L = biquin, all of the $R_3EM(CO)_3L$ complexes exhibit emission from the lowest excited state at 77 K in solution and some of the Re complexes exhibit emission from the lowest excited state at 298 K in fluid solution (Table IV). The 298 K emission is in the ~10^{-6} s lifetime regime with a quantum yield of ~10^{-3}. At 298 K the emission spectrum, lifetime, and quantum yield are independent of the exciting wavelength for λ_{ex} longer than 300 nm. We associate the emission with the (E–M)σ_b → π*L CT excited state.

Emission at 77 K is more efficient and longer lived than at 298 K. Further, there is a rather significant blue-shift and sharpening of the emission spectrum for those complexes that are emissive

(8) Morse, D. L.; Wrighton, M. S. *J. Am. Chem. Soc.* **1976**, *98*, 3931.
(9) Higginson, B. R.; Lloyd, D. R.; Evans, S.; Orchard, A. F. *J. Chem. Soc., Faraday Trans. 2* **1975**, *71*, 1913.
(10) Hall, M. B. *J. Am. Chem. Soc.* **1975**, *97*, 2057.
(11) Wrighton, M. S.; Morse, D. L.; Pdungsap, L. *J. Am. Chem. Soc.* **1975**, *97*, 2073.

Table IV. Emission Properties of $R_3ERe(CO)_3L$

complex	temp, K	solvent	band max, cm^{-1} (nm)	width at half-height, cm^{-1}	lifetime τ (±10%), μs	quantum yield,[a] Φ (±20%)
$Ph_3SnRe(CO)_3(phen)$	298	EPA	13 300 (~750)	3200	1.8	2×10^{-3}
	77	EPA	15 700 (~635)	2600	120	0.3
$Ph_3GeRe(CO)_3(phen)$	298	EPA	13 000 (~770)	3200	2.6	3×10^{-3}
	77	EPA	15 200 (~660)	2600	110	0.3
$Ph_3SnRe(CO)_3(bpy)$	298	EPA	13 700 (~730)	3200		
	77	EPA	15 900 (~630)	2500	90	
$Me_3SnRe(CO)_3(phen)$	77	EPA	14 400 (~695)	2400	70	0.06
$Ph_3SnMn(CO)_3(phen)$	77	EPA	17 500 (~570)	2200	~0.4	6×10^{-4}
$Ph_3GeMn(CO)_3(phen)$	77	EPA	16 700 (~600)	2600	~0.4	6×10^{-4}

[a] Band maximum and quantum yield are those measured for the isoabsorbance point in the optical absorption spectra of each complex at 298 and 77 K. For details see Experimental Section.

Table V. Excitation Wavelength Dependence of Emission Band Maximum for Re Complexes at 77 K

complex	solvent	λ_{excit}, nm	λ_{emis},[a] nm
$Ph_3GeRe(CO)_3(phen)$	EPA	≤400	618
		420	620
		480	628
		500	628
	MTHF	≤370	615
		420	620
		440	625
		470	640
		480	650
		490	655
		500	655
	solid	*b*	620
$Ph_3SnRe(CO)_3(phen)$	EPA	≤440	605
		480	625
		500	630
	MTHF	≤400	605
		440	610
		480	630
		500	640
	solid	*b*	590
$Me_3SnRe(CO)_3(phen)$	EPA	≤450	665
		500	675
		540	685
	MTHF	≤450	665
		500	675
		540	685
$(CO)_5ReRe(CO)_3(phen)$	EPA	≤500	665
		520	675
		540	685
$Ph_3SnRe(CO)_3(bpy)$	EPA	≤420	605
		460	615
		480	625
		500	635

[a] Uncorrected emission band maximum recorded on PE Model MPF 44. [b] Independent of λ_{excit} over the excitation wavelength range 320-500 nm.

at 298 K. Such large spectral changes accompanying changes in solvent rigidity and in temperature are well documented.[3,6,7] But we now note that the low-temperature emission is also somewhat sensitive to the excitation wavelength (Table V). The width of the emission is insensitive to the excitation wavelength, but there is a definite effect on the emission maximum. As shown in Table V, the pure solid exhibits no such excitation wavelength effect on the emission maximum and the magnitude of the effect in solution depends on the solvent used. On the basis of an effect from solvent, we propose that the excitation wavelength effects are due to selective excitation of complexes in one of several environments. Data in Table I already establish a strong environmental effect on the $(E-M)\sigma_b \rightarrow \pi^*L$ CT. Apparently, the 77 K rigid media allow various complex/solvent arrangements to be frozen, giving rise to a distribution of sites yielding different excited-state energies.

Another interesting finding is that the Mn complexes are emissive. Note, however, that the quantum yields and lifetimes are very low compared to those of the Re species. The emission energy

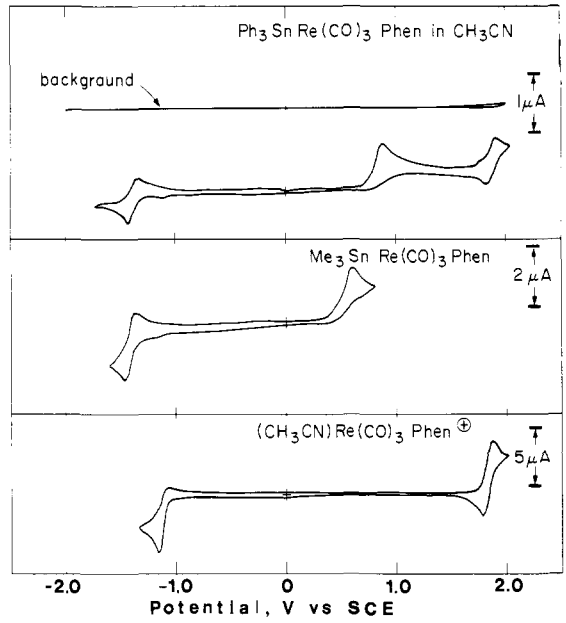

Figure 2. Cyclic voltammograms of representative complexes at 100 mV/s at 298 K in deoxygenated 0.1 M $[n\text{-}Bu_4N]ClO_4$ solutions. Note that the second, reversible oxidation for $Ph_3SnRe(CO)_3(phen)$ is in fact associated with the product from the first (irreversible) oxidation. The oxidation product from $Ph_3SnRe(CO)_3(phen)$ is $[(CH_3CN)Re(CO)_3(phen)]^+$ characterized in the bottom frame.

is insensitive to excitation wavelength, unlike the Re species. The most interesting fact, though, is that the Mn complexes emit at an energy higher than that of the Re analogues (Table IV), while the Re complexes show a higher energy first absorption. The emissions of the Mn complexes strongly overlap the absorption, whereas in Re there is little overlap. The Re complexes are longer lived than the Mn. Taken as a whole, the data suggest that the Mn complexes are emissive from the singlet excited state, whereas the Re complexes emit from a triplet state. This hypothesis and the excitation wavelength dependence of the Re complexes deserves further evaluation, but these are not the focus of the present work and will be dealt with in a subsequent report.

The detectable luminescence from the $(E-Re)\sigma_b \rightarrow \pi^*L$ CT excited state at 298 K provides an extremely useful spectroscopic handle for gaining insight into the photochemistry of these complexes. First, from the emission spectrum one obtains a direct measure of the energy of the excited state compared to the ground state. Second, from the emission lifetime it is possible to determine how long the excited species will persist. Third, the emission allows a probe of bimolecular excited-state processes, by following its quenching.

(d) Electrochemistry and Oxidation of $R_3EM(CO)_3L$. The ground-state redox properties of the $R_3EM(CO)_3L$ complexes have been studied by using cyclic voltammetry in deoxygenated, dry CH_2Cl_2 or CH_3CN solutions of 0.1 M $[n\text{-}Bu_4N]ClO_4$. In all cases we find that the $R_3EM(CO)_3L$ species can be reversibly reduced by one electron. Figure 2 shows representitive cyclic voltam-

Table VI. Electrochemical Data for Ground State of $R_3EM(CO)_3L$[a]

complex	potential in V vs. SCE: E_{PA} - [$R_3EM(CO)_3L)^{+\cdot}$/ $R_3EM(CO)_3L$][b]	$E_{1/2}$ - [$R_3EM(CO)_3L$/ ($R_3EM(CO)_3L)^{-\cdot}$]
$Ph_3SnRe(CO)_3(phen)$	+0.82	−1.40
$Ph_3GeRe(CO)_3(phen)$	+0.85	−1.42
$Me_3SnRe(CO)_3(phen)$	+0.52	−1.44
$Ph_3SnRe(CO)_3(bpy)$	+0.78	−1.47
$Ph_3SnRe(CO)_2(biquin)$[c]	+0.80	−1.08
$(OC)_5ReRe(CO)_3(phen)$	+0.62	−1.45
$Ph_3GeMn(CO)_3(phen)$	+0.53	−1.67
$ClRe(CO)_3(bpy)$[d]	+1.35	−1.41
$ClRe(CO)_3(phen)$[d]	+1.33	−1.35
$ClRe(CO)_3(biquin)$[d]	+1.40	−1.15
phen[d,e]		−2.12
bpy[d,e]		−2.24
biquin[d,e]		−1.82

[a] Measurements were made in 0.1 M [n-Bu_4N]ClO_4, CH_3CN solution unless otherwise indicated. [b] Anodic peak potential measured at a scan rate of 100 mV/s. [c] Measured in 0.1 M [n-Bu_4N]PF_6, CH_2Cl_2 solution. This compound shows a second, reversible reduction at −1.68 V vs. SCE. [d] Data from ref 13. [e] Free ligands.

mograms revealing a reversible wave at a fairly negative potential and logically associated with the π^*L LUMO. A list of the complexes and the values of $E_{1/2}(R_3EM(CO)_3L/(R_3EM(CO)_3L^{-\cdot})$ are given in Table VI. The reversible reduction accords well with findings for other metal–carbonyl complexes of L generally[12,13] and, specifically, is consistent with the one-electron diagram in Scheme II. Addition of an electron to the π^*L LUMO is not expected to lend dissociative lability to the complex. The ligands themselves are reversibly reducible, and coordination via the N lone pair is not likely to lead to substantially different behavior. Finally, the reduction wave appears at a potential that is not too different from that for $ClRe(CO)_3L$, also a neutral rhenium–carbonyl complex of L.[12,13]

In sharp contrast to the reduction behavior we find that the oxidation of the $R_3EM(CO)_3L$ species is irreversible by cyclic voltammetry and scan rates of even 50 V/s yield no evidence of a persistent $(R_3EM(CO)_3L)^{+\cdot}$. Under the same conditions we find some reversibility for the oxidation of $ClRe(CO)_3L$. Further, the oxidation peak for the $R_3EM(CO)_3L$ complexes is at a significantly less positive potential than for the $ClRe(CO)_3L$ analogues (Table VI). Also, $Me_3SnRe(CO)_3(phen)$ is oxidized at a less positive potential than the Ph_3Sn- species, consistent with the lower energy CT energy for the Me_3Sn- species. Continuation of the cyclic voltammogram beyond the potential of the oxidation peak reveals a reversible oxidation wave at ~+1.8 V vs. SCE (Figure 2) in CH_3CN solution. This reversible oxidation wave must be associated with the oxidation of the product formed from oxidation of $R_3EM(CO)_3L$. The reversible oxidation wave is in the position identical with that found for an authentic sample of *fac*-$[(CH_3CN)M(CO)_3L]^+$. Further, a small wave at ~−1.2 V vs. SCE, found only when the scan direction is first positive, is attributable to *fac*-$[(CH_3CN)M(CO)_3L]^+$ formed from oxidation of $R_3EM(CO)_3L$. Controlled potential oxidation of $R_3EM(CO)_3L$ results in quantitative generation of *fac*-$[(CH_3CN)M(CO)_3L]^+$ on the basis of the $R_3EM(CO)_3L$ starting material. The product was fully characterized by infrared, NMR, and UV–vis spectroscopy by comparison to an authentic sample. Chemical oxidation of $R_3EM(CO)_3L$ with Ce^{4+} from $(NH_4)_2Ce(NO_3)_6$ in CH_3CN solution also yields a quantitative conversion to *fac*-$[(CH_3CN)M(CO)_3L]^+$.

The cyclic voltammetry indicates that the next oxidation involves more than one electron per $R_3EM(CO)_3L$ molecule. Controlled potential oxidation at a potential positive of the anodic peak for quiet solutions shows an approximate two-electron process, but oxidation in stirred solution shows less than two electrons per molecule consumed. We propose that the first step is according to eq 6 and that a rapid dissociation according to eq 7 occurs to

$$R_3EM(CO)_3L \xrightarrow{-e^-} [R_3EM(CO)_3L]^{+\cdot} \quad (6)$$

$$[R_3EM(CO)_3L]^{+\cdot} \xrightarrow{k_7} R_3E\cdot + [M(CO)_3L]^+ \quad (7)$$

yield a 16-valence electron M-centered species that can rapidly react with a donor solvent such as CH_3CN according to eq 8 to

$$[M(CO)_3L]^+ + CH_3CN \xrightarrow{\text{fast}} fac\text{-}[(CH_3CN)M(CO)_3L]^+ \quad (8)$$

yield an inert, isolable, 18-valence electron species. The $R_3E\cdot$ species can couple or be oxidized, accounting for the approximate two-electron process for quiet solutions and a less than two-electron oxidation for stirred solutions where the $R_3E\cdot$ species is swept away from the vicinity of the electrode.

Cleavage of $[R_3EM(CO)_3L]^{+\cdot}$ in the manner indicated in eq 7 is supported by the chemical oxidation of $Ph_3SnRe(CO)_3(phen)$ by $[Fe(\eta^5\text{-}C_5H_5)_2]^+$. The rate of oxidation by $[Fe(\eta^5\text{-}C_5H_5)_2]^+$ is slow; complete reaction at 298 K in CH_3CN requires several hours at $\sim 10^{-3}$ M $Ph_3SnRe(CO)_3(phen)$ and $\sim 10^{-2}$ M $[Fe(\eta^5\text{-}C_5H_5)_2]^+$. The slow rate is presumably due to the fact that the E° for $[Fe(\eta^5\text{-}C_5H_5)_2]^{+/0}$ is only +0.4 V vs. SCE[14] and is somewhat more negative than the anodic peak in the cyclic voltammetry of the $R_3EM(CO)_3L$ species. The Re-containing product is *fac*-$[(CH_3CN)Re(CO)_3(phen)]^+$ and is formed in a molar amount equal to the number of moles of $[Fe(\eta^5\text{-}C_5H_5)_2]^+$ consumed in the reaction. Further, Ph_6Sn_2, presumably from coupling of $Ph_3Sn\cdot$, is the infrared-detected, Sn-containing product.[15] Apparently, $[Fe(\eta^5\text{-}C_5H_5)_2]^+$ is incapable of oxidizing $Ph_3Sn\cdot$ at a rate that competes with the coupling to form Ph_6Sn_2.

Chemical oxidation of $Ph_3SnRe(CO)_3(phen)$ by Ce^{4+} from $(NH_4)_2Ce(NO_3)_6$ in CH_3CN solution also leads to *fac*-$[(CH_3CN)Re(CO)_3(phen)]^+$ as the Re-containing product, but the reaction is fast. Even when the Ce^{4+} is added slowly, we find that formation of *fac*-$[(CH_3CN)Re(CO)_3(phen)]^+$ consumes 2 equiv of Ce^{4+}. In this case we find that the principal Sn-containing product is $(Ph_3Sn)_2O$ as determined by infrared.[15] The oxide likely forms via oxidation of the $Ph_3Sn\cdot$ followed by reaction with traces of H_2O in the solvent or by the room-temperature decomposition of Ph_3SnONO_2.[16] Curiously, Ce^{4+} oxidation of $Ph_3GeRe(CO)_3(phen)$ under the same conditions only consumes 1 equiv of Ce^{4+} per *fac*-$[(CH_3CN)Re(CO)_3(phen)]^+$ formed. By infrared the Ge-containing product appears to be $(Ph_3Ge)_2O$.[15] This product could be formed via reaction of $Ph_3Ge\cdot$ with traces of H_2O in the solvent. The one-electron oxidation of the Ge species to yield *fac*-$[(CH_3CN)Re(CO)_3(phen)]^+$ provides further support for cleavage in the manner indicated in eq 7. Oxidation of the previously studied[8] $(OC)_5ReRe(CO)_3(phen)$ by either Ce^{4+} or $Fe(phen)_3^{3+}$ requires two equivalents to give $[Re(CO)_5(CH_3CN)]^+$ and *fac*-$[(CH_3CN)Re(CO)_3phen]^+$ in quantitative yield.

The lack of any detectable reduction current in the cyclic voltammogram after the potential is switched after the anodic peak, even at scan rates of 50 V/s, suggests that the dissociation rate constant, k_7, is fairly large and at least 10^3 s^{-1}. Our earlier report on the photochemistry of $Ph_3ERe(CO)_3(phen)$ showed an E–Re cleavage rate of $\sim 10^5$ s^{-1} upon excitation of an electron from the (E–Re)σ_b level.[3] The one-electron oxidation, eq 6, thus logically involves removal of an electron from the HOMO, (E–Re)σ_b, and cleavage of the E–Re bond should occur at a similar rate as found upon excitation corresponding to the (E–Re)$\sigma_b \rightarrow \pi^*$phen CT transition.[3] Scheme III summarizes the electro-

(12) Luong, J. C.; Nadjo, L.; Wrighton, M. S. *J. Am. Chem. Soc.* **1978**, *100*, 5790.
(13) Fredericks, S. M.; Wrighton, M. S., to be submitted for publication.
(14) Janz, G. J.; Tomkins, R. P. T. "Nonaqueous Electrolyte Handbook"; Academic Press: New York, 1973; Vol. II.
(15) (a) "Sadtler Standard Spectra=Organometallics IR Grating Spectra"; Sadtler Research Laboratories, Inc.: 1970, Vol. I. (b) Kushlefsy, B.; Simmons, I.; Ross, A. *Inorg. Chem.* **1963**, *2*, 187.
(16) Coates, G. E.; Green, M. L. H.; Wade, K. "Organometallic Compounds", 3rd ed.; Methuen: London, Vol. I.

Scheme III. Summary of Ground-State Electrochemistry for $R_3EM(CO)_3L$ for R = Ph, E = Sn and Ge, and L = 1,10-Phenanthroline

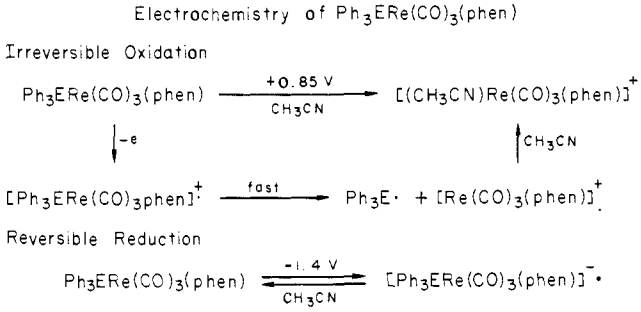

chemistry of $Ph_3ERe(CO)_3(phen)$.

(e) Photochemistry of $R_3EM(CO)_3L$. As we have previously communicated,[3] $R_3EM(CO)_3L$ are photosensitive molecules in solution, eq 9 and 10. Even the molecules that are emissive in

$$Ph_3E\text{–}Re(CO)_3(phen) \xrightarrow{h\nu} [Ph_3E^+\text{—}Re(CO)_3(phen)^-]^* \quad (9)$$

$$[Ph_3E^+\text{—}Re(CO)_3(phen)^-]^* \xrightarrow{k_{10}} Ph_3E\cdot + [Re(CO)_3(phen)]\cdot \quad (10)$$

solution undergo reaction and in fact it is the emission that allowed us to evaluate the dissociation rate constant k_{10} from the photoexcited species. The electrochemistry and redox reactions described above provide support for the claim that the photoexcited species cleaves such that the $R_3E\cdot$ (rather than R_3E^+) forms. If the R_3E– group leaves as the neutral radical from $[R_3EM(CO)_3L]^+\cdot$, it is very likely that the R_3E– species will leave as a neutral fragment from the excited complex, since the excited electron is localized mainly on the L acceptor ligand.

Our new results concerning the photochemistry of $R_3EM(CO)_3L$ relate to the species having relatively long-lived excited states in solution where bimolecular processes are possible. Specifically, we have examined the excited-state electron-transfer processes represented by eq 11 and 12. We find that a number

$$[Ph_3E^+\text{—}Re(CO)_3(phen)^-]^* + Q \xrightarrow{k_{11}} [Ph_3E\text{–}Re(CO)_3(phen)]^{-}\cdot + Q^+ \quad (11)$$

$$[Ph_3E^+\text{—}Re(CO)_3(phen)^-]^* + P^+ \xrightarrow{k_{12}} [Ph_3E\text{–}Re(CO)_3(phen)]^{+}\cdot + P \quad (12)$$

of electron-donor quenchers, Q, and electron-acceptor quenchers, P^+, quench the photoexcited emission of the Re complexes in CH_3CN/0.1 M $[n\text{-}Bu_4N]PF_6$ at 298 K with Stern–Volmer kinetics. For a number of quenchers the quenching constants k_{11} and k_{12} are very high and approach the diffusion-controlled limit. Figure 3 shows a summary of the quenching constants as a function of $E_{1/2}(Q^+/Q)$ and $E_{1/2}(P^+/P)$ for the $Ph_3SnRe(CO)_3(phen)$ complex. The data show that k_{11} is nearly diffusion controlled for $E_{1/2}(Q^+/Q)$ more negative than ~+0.2 V vs. SCE and that k_{12} is nearly diffusion controlled for $E_{1/2}(P^+/P)$ more positive than −1.0 V vs. SCE.

All of the quenchers investigated are fast, one-electron systems where variation in k_{11} or k_{12} should only be a consequence of the energetics for the redox process. The excited $R_3EM(CO)_3L$ species is a much more powerful oxidant and simultaneously a much more powerful reductant than the ground state (Scheme I). The excited-state energy is taken to be a good measure of the increase in oxidation and reduction power of the excited state relative to the ground state. The emission of the complexes provides a direct measure of the excited-state energy, but since the emission spectrum is broad and structureless, there is still some ambiguity as to what value to assign to the excited-state energy. We arbitrarily take the excited-state energy to be that point on the high-energy side of the 298 K emission spectrum where the emission intensity has reached 10% of the maximum intensity.

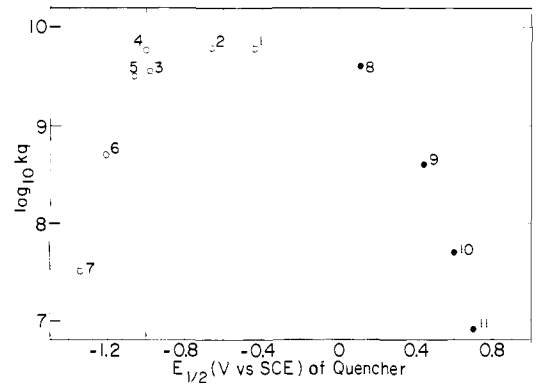

Figure 3. Plot of log k_q, the emission quenching rate constant vs. $E_{1/2}$, the redox potential of quencher. Plot of log k_q vs. $E_{1/2}$ for the emission quenching rate constant of $Ph_3SnRe(CO)_3(phen)$ in degassed CH_3CN solution of $[n\text{-}Bu_4N]PF_6$ at 298 K by various quenchers. The open circles are for oxidizing quenchers (oxidized form of redox couple present) and the closed circles are for reducing quenchers (reduced form of redox couple present). The numbers identify the quenchers with the corresponding $E_{1/2}$ value determined in this laboratory by cyclic voltammetry: (1) *N,N'*-dimethyl-4,4'-bipyridinium hexafluorophosphate ($E_{1/2}$ = −0.44 V); (2) *N*-methyl-4-cyanopyridinium hexafluorophosphate ($E_{1/2}$ = −0.66 V); (3) *N*-methyl methylisonicotinate hexafluorophosphate ($E_{1/2}$ = −0.78 V); (4) 4,4'-dinitrophenyl ($E_{1/2}$ = −1.00 V); (5) 4-chloronitrobenzene ($E_{1/2}$ = −1.06 V); (6) 4-methylnitrobenzene ($E_{1/2}$ = −1.21 V); (7) 4-aminonitrobenzene ($E_{1/2}$ = −1.34 V); (8) *N,N,N',N'*-tetramethyl-*p*-phenylenediamine ($E_{1/2}$ = +0.11 V); (9) *N,N'*-diphenyl-*p*-phenylenediamine ($E_{1/2}$ = +0.44 V); (10) phenothiazine ($E_{1/2}$ = +0.60 V); (11) *N,N*-dimethyl-*p*-toluidine ($E_{1/2}$ = +0.70 V).

This value along with the ground-state values for $E_{1/2}[R_3EM(CO)_3L]^{+/0/-}$ can be used to determine the formal potentials for the excited species. Since the $[R_3EM(CO)_3L]^{0/-}$ couple is reversible, the associated $E_{1/2}$ can be taken to be that from the cyclic voltammetry (Table VI). The $[R_3EM(CO)_3L]^{+/0}$ system is not reversible and the cyclic voltammetry only establishes that the associated $E_{1/2}$ is more negative than the anodic peak. But since there is no reason to expect the heterogeneous oxidation kinetics to be slow (homogeneous reaction is fast), we take $E_{1/2}[R_3EM(CO)_3L]^{+\cdot/0/-\cdot}$ to be closely approximated by the position of the anodic peak in the cyclic voltammogram (about 50 mV more negative than the anodic peak). The redox energetics for $Ph_3ERe(CO)_3(phen)$, culled from emission spectroscopy and cyclic voltammetry, are summarized in Scheme IV. The energetics accord well with the data given in Figure 3: when excited-state electron transfer is significantly energetically downhill, the quenching is fast, but when the energetics are less favorable, the quenching constants decline. Such plots have previously been found[12] for quenching of excited *fac*-$[XRe(CO)_3(phen)]$ and for numerous excited organic molecules[17] and for excited $Ru(bpy)_3^{2+}$ and related inorganic complexes.[18-20]

An interesting aspect of the excited-state electron-transfer quenching is that quenching via eq 11, electron donation to the excited state, does not lead to net redox reaction for the fast, reversible one-electron donors used, but quenching according to eq 12 does lead to net redox reaction. Quenching according to eq 12 involves one-electron oxidation of the Re complex to form $[Ph_3ERe(CO)_3(phen)]^{+}\cdot$ that is now known to dissociate rapidly. The reductive quenching, eq 11, generates $[Ph_3ERe(CO)_3(phen)]^{-}\cdot$ that is reversibly produced in cyclic voltammetry scans as slow as 20 mV/s and apparently does not undergo rapid dissociative chemistry. Table VII summarizes some photoredox quantum yields for reaction in CH_3CN solution where sufficient concentration of quencher is present to quench all of the excited species. Reductive quenching (e.g., TMPD) results in very little net

(17) Rehm, D.; Weller, A. *Ber. Bunsenges. Phys. Chem.* **1969**, *73*, 834.
(18) Bock, C. R.; Meyer, T. J.; Whitten, D. G. *J. Am. Chem. Soc.* **1975**, *97*, 2909.
(19) Sutin, N.; Creutz, C. *Adv. Chem. Ser.* **1978**, *No. 168*, 1.
(20) (a) Whitten, D. G. *Acc. Chem. Res.* **1980**, *13*, 83. (b) Balzani, V.; Bolletta, F.; Scandola, F.; Ballardini, R. *Pure Appl. Chem.* **1979**, *51*, 299.

Table VII. Net Electron-Transfer Quantum Yield for $R_3ERe(CO)_3(phen)$ at 25 °C in CH_3CN

complex	quencher (no),[a] concn (M)	λ_{irrad}[b]	Φ ± 10% ($X^c < 3) \times 10^{-5}$ M	Φ ± 10% ($X^c < 8) \times 10^{-5}$ M
$Ph_3SnRe(CO)_3(phen)$	PQ^{2+} (1), 2.4×10^{-3}	458	0.33	0.16
	PQ^{2+} (1), 2.4×10^{-3}	473	0.25	0.10
	4,4'-dinitrobiphenyl (4), 4×10^{-3}	476		0.08
	TMPD (8), 4.3×10^{-2}	476		$<10^{-3}$
	N,N'-diphenyl-*p*-phenylenediamine (9), 3×10^{-3}	476		$<10^{-3}$
$Ph_3GeRe(CO)_3(phen)$	PQ^{2+} (1), 2.8×10^{-3}	436		0.08
	PQ^{2+} (1), 2.8×10^{-3}	458	0.12	0.07
	PQ^{2+} (1), 2.8×10^{-3}	473	0.19	0.08
$Me_3SnRe(CO)_3(phen)$	PQ^{2+} (1), 2.7×10^{-3}	473		2.0
	PQ^{2+} (1), 3.8×10^{-2}	488		1.8
	TMPD (8), 5.8×10^{-2}	473		$<10^{-3}$

[a] These numbers correspond to those in Figure 3. [b] Wavelength of irradiation. [c] The concentration of product ($PQ^{+}\cdot$) present at the end of the measurement. The Re product is $[(CH_3CN)Re(CO)_3(phen)]^+$.

Scheme IV. Approximate Redox Energetics for Ground and Excited States of $Ph_3ERe(CO)_3(phen)$, (the Quenching Systems $PQ^{2+/+\cdot}$ (No. 1 in Figure 3) and $TMPD^{+\cdot/0}$ (No. 8 in Figure 3) Are Included for Comparison)

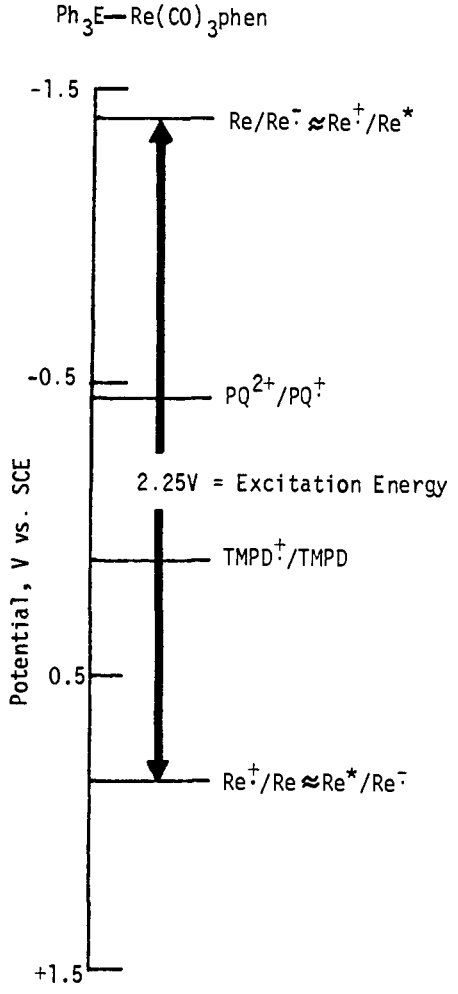

photoredox. But as can be seen, the oxidative quenching results in high initial quantum yields for disappearance of the $Ph_3ERe(CO)_3(phen)$. Quenching using PQ^{2+} results in the formation of *fac*-$[(CH_3CN)Re(CO)_3(phen)]^+$ and $PQ^{+}\cdot$ in a 1/1 ratio. The 1/1 ratio provides further evidence that eq 7 and 8 represent the course of events following formation of $[Ph_3ERe(CO)_3(phen)]^{+}\cdot$. Flash photolysis on the 10-μs scale of $Ph_3GeRe(CO)_3(phen)$ in the presence of sufficient PQ^{2+} to quench all emission shows little evidence for back-reaction of $PQ^{+}\cdot$ once it is formed; this result suggests that the lack of unit quantum efficiency is due to a significant efficiency for back-reaction in the geminate cage.

Flash photolysis of $[Ph_3ERe(CO)_3(phen)]$ in the presence of an amount of TMPD sufficient to quench all excited states provides direct evidence for the reductive quenching (eq 13). The

$$[Ph_3E^+—Re(CO)_3(phen)^-]^* + TMPD \xrightarrow{k_{13}} [Ph_3ERe(CO)_3(phen)]^-\cdot + TMPD^+\cdot \quad (13)$$

$TMPD^{+}\cdot$ was detected by using a 632.8-nm probe beam absorbed by the intermediate $TMPD^{+}\cdot$. The $TMPD^{+}\cdot$, however, is only generated as a transient and since little or no net chemical change is found, back-reaction, eq 14, apparently occurs. With the as-

$$[Ph_3ERe(CO)_3(phen)]^-\cdot + TMPD^+\cdot \xrightarrow{k_{14}} Ph_3ERe(CO)_3(phen) + TMPD \quad (14)$$

sumption of bimolecular, equal concentration kinetics, the decay of the $TMPD^{+}\cdot$ can be used to evaluate k_{14}. We find k_{14} to be $>10^8$ M^{-1} s^{-1}. The large value for k_{14} is reasonable in view of the large driving force for the back-reaction (see Scheme IV) and the fast, one-electron systems involved.

Note that the quantum yields for photoreaction via oxidative quenching are very high initially but decline significantly as reaction proceeds. The high initial quantum yields suggest good efficiency for cage escape of the primary electron-transfer products. The declining quantum yields suggest that photoproducts are somehow quenching reaction. There are several possible consequences of product formation: (i) competitive light absorption, (ii) reductive electron-transfer quenching of the excited species and (iii) enhanced rate of electron back-transfer. For experiments using PQ^{2+} as the oxidative quencher, we chose an irradiation wavelength where the absorption of light by $PQ^{+}\cdot$ is at a minimum; the absorption of $PQ^{+}\cdot$ is trivially small at the extent conversions where photoreaction quantum yields are significantly attenuated. Reductive quenching by $PQ^{+}\cdot$ is unimportant because it can quench with a rate constant no faster than diffusion controlled which is what is found for oxidative quenching by PQ^{2+}. Thus, the fraction of $[Ph_3ERe(CO)_3(phen)]$ excited states quenched by the photoproduct, $PQ^{+}\cdot$, is just the ratio $PQ^{+}\cdot/PQ^{2+}$ which is very small.

The possibility that back-reaction occurs as represented by eq 15 remains. Taking k_{15} to be $\sim 5 \times 10^9$ M^{-1} s^{-1}, the rate of

$$[Ph_3ERe(CO)_3(phen)]^{+}\cdot + PQ^+\cdot \xrightarrow{k_{15}} Ph_3ERe(CO)_3(phen) + PQ^{2+} \quad (15)$$

reaction according to eq 15 is given by eq 16. Process 15 occurs

$$\text{rate of process 15} = (5 \times 10^9)[PQ^+\cdot][Ph_3ERe(CO)_3(phen)^+\cdot] \quad (16)$$

in competition with the E–Re cleavage represented by eq 7 which has a rate given by eq 17. Thus, chemistry according to eq 15

$$\text{rate of process 7} = k_7[Ph_3ERe(CO)_3(phen)^+\cdot] \quad (17)$$

attenuates the observed photoreaction quantum yields when the product $(5 \times 10^9)[PQ^+\cdot]$ becomes sizable compared to k_7. The cyclic voltammetry indicates k_7 to be $\geq 10^3$ s^{-1} and the photo-

Scheme V. Summary of Excited-State Redox Processes of $Ph_3ERe(CO)_3(phen)$

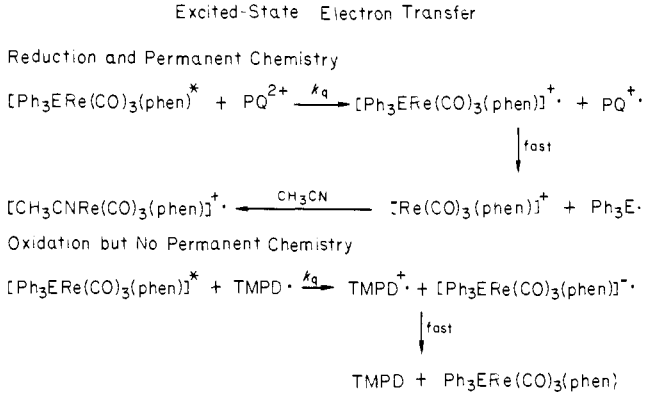

chemistry[3] suggests k_7 to be $\sim 10^5\ s^{-1}$. We find $[PQ^+\cdot]$ in the range of 10^{-5} M to be able to attenuate photoreaction quantum yields consistent with k_7 in the range of $10^5\ s^{-1}$. thus, the data are internally consistent. Scheme V summarizes the excited-state electron-transfer processes of $Ph_3ERe(CO)_3(phen)$.

The photochemistry of $Me_3SnRe(CO)_3(phen)$ has been investigated in $CHCl_3$, and as for the $Ph_3ERe(CO)_3(phen)$ we find clean, efficient formation of $ClRe(CO)_3(phen)$ upon photoexcitation. The quantum yield at 488 nm is 0.2 ± 0.02. The $Me_3SnRe(CO)_3(phen)$ is not detectably emissive under these conditions, and a rate constant for Sn–Re dissociation cannot be directly determined as was done for the Ph_3E– species. However, TMPD does quench the formation of the $ClRe(CO)_3(phen)$, presumably via electron-transfer quenching of the $(Sn–Re)\sigma_b \rightarrow \pi^*$phen CT excited state. For example, $\sim 10^{-2}$ M TMPD in $CHCl_3$ attenuates the disappearance quantum yield by 1 order of magnitude. With the assumption that TMPD quenches the excited Me_3Sn– species at the same rate as it quenches $Ph_3SnRe(CO)_3(phen)$ (Figure 3), the lifetime of the excited $Me_3SnRe(CO)_3(phen)$ species is $\sim 10^{-7}$ s. With a quantum yield of 0.2 for formation of $ClRe(CO)_3(phen)$ we conclude that k_{10} for $Me_3SnRe(CO)_3(phen)$ is $\sim 10^6\ s^{-1}$ or somewhat higher than for $Ph_3ERe(CO)_3(phen)$. Excitation of $Me_3SnRe(CO)_3(phen)$ in the presence of PQ^{2+} (Table VII) gives a very high quantum yield for $PQ^{+}\cdot$ formation. Presumably, this $\Phi \approx 2.0$ results from first forming $PQ^{+}\cdot$ by excited-state reduction followed by reduction of a second PQ^{2+} in a ground-state reaction with a fragment ($\cdot SnMe_3$) from the $[Me_3SnRe(CO)_3(phen)]^{+}\cdot$. The higher quantum efficiency for $PQ^{+}\cdot$ formation using the Me_3Sn– vs. Ph_3E– complexes is consistent with a higher value of k_{10} and k_7 for the Me_3Sn– species. Detailed studies of the species that are not luminescent in solution will require use of fast time scale flash photolysis.

Summary

Complexes of the general formula $R_3EM(CO)_3L$ have a low-lying charge-transfer excited state whose energy depends on L, M, and R_3E– in a manner consistent with (E–M) → L charge transfer. Chemical, electrochemical, and bimolecular excited-state electron-transfer processes suggest that the HOMO has sigma E–M bonding character and that the LUMO is mainly localized on L for the systems studied. Removal of an electron from the HOMO induces E–M bond lability such that E–M dissociation occurs with a rate constant of $\sim 10^5\ s^{-1}$, while addition of an electron to the LUMO does not result in E–M bond lability on the time scale of slow cyclic voltammetry (20 mV/s) or the time required for electron back-transfer involving the primary excited-state electron-transfer products, e.g., $TMPD^{+}\cdot$ and $[Ph_3GeRe(CO)_3(phen)]^{-}\cdot$.

Experimental Section

Spectroscopic Measurements. UV–vis spectra were recorded by using a Cary 17 spectrophotometer; IR spectra were recorded on a Perkin-Elmer 180 spectrophotometer; and emission spectra were recorded by using a Perkin-Elmer MPF 44. Emission lifetimes were measured by using as an excitation source a rhodamine dye laser (560 nm, ~5-nm pulse width) or a Xenon Corporation Model 437 nanopulser filtered to pass light of wavelength 436 nm < λ < 580 nm for room-temperature measurements or filtered to pass UV light for low-temperature measurements. The detection unit includes a TRW Instruments decay time fluorometer with output to an oscilloscope. Emission intensity vs. time was recorded by photographing the oscilloscope trace with a Polaroid camera.

Chemicals. Acetonitrile (spectral grade, Eastman Chemical Co.) and CH_2Cl_2 (reagent grade) were dried by distillation over P_2O_5 under Ar. Tetrahydrofuran (THF) was distilled from sodium benzophenone ketyl under Ar. $[n\text{-}Bu_4N]ClO_4$ (electrometric grade, from Southwestern Analytical Chemicals, Inc.) was vacuum dried at 70 °C for 24 h. $[n\text{-}Bu_4N]PF_6$ was prepared by metathesis of $[n\text{-}Bu_4N]Br$ (Pfaltz and Bauer Co.) and NH_4PF_6 (Alfa Ventron) in hot acetone; the $[n\text{-}Bu_4N]PF_6$ precipitates upon addition of water. The $[n\text{-}Bu_4N]PF_6$ was recrystallized from EtOH. All quenchers used in emission quenching measurements have been reported previously.[12]

$Re_2(CO)_{10}$ and $Mn_2(CO)_{10}$ were purchased from Strem Chemical, Inc., and used without further purification. $BrRe(CO)_5$ was prepared according to the literature method.[21] A CCl_4 solution of Br_2 was added dropwise to a stirred CCl_4 solution of $Re_2(CO)_{10}$. About 10 min later, the solution turned cloudy and the dropwise addition was continued until a brown-red color persisted in the reaction mixture. The off-white precipitate was collected, washed with CCl_4, and recrystallized from CH_2Cl_2/isooctane to give crystalline $BrRe(CO)_5$. Purity was confirmed by IR spectroscopy in the CO stretching region. $BrMn(CO)_5$ was prepared similarly except it was synthesized under Ar.

$BrRe(CO)_3L$ and $BrMn(CO)_3L$ were prepared from $BrRe(CO)_5$ and $BrMn(CO)_5$, respectively, with the appropriate ligand, L = 1,10-phenanthroline (G. Frederick Smith Chemical Co.), 2,2′-bipyridine (Baker), and 2,2′-biquinoline (Aldrich) according to the method described earlier.[7] The synthetic procedures for preparation of $(CO)_5ReRe(CO)_3(phen)$[8] and $[(CH_3CN)Re(CO)_5]^{+}$[22] have been previously described.

Ph_3SnCl (Alfa) was recrystallized from CH_2Cl_2/isooctane. Ph_3GeBr and Me_3SnCl (Alfa) and $AgOSO_2CF_3$ (Aldrich) were used as received. Ceric ammonium nitrate (G. Frederick Smith) was used as received. $[Fe(phen)_3](PF_6)_3$[23a] and $[Fe(\eta^5\text{-}C_5H_5)_2]PF_6$[23b] were prepared according to the published methods.

Synthesis of $R_3EM(CO)_3L$[3] (R = Ph, Me; E = Sn, Ge; M = Mn, Re; L = phen, bpy, biquin). The synthesis of these complexes was carried out under Ar by using Schlenk techniques. A typical synthetic procedure was carried out as follows: 4 mL of 1% Na/Hg was added through a three-way stopcock to a THF suspension of 1.0 g (1.88×10^{-3} mol) of $BrRe(CO)_3(phen)$. The solution immediately turned greenish then deep blue after 2 h of continuous stirring. The excess Na/Hg was removed by draining through a vacuum stopcock attached near the bottom of the reaction flask. Then 0.73 g (1.88×10^{-3} mol) of Ph_3SnCl in 20 mL of THF was added dropwise via a cannula during which time the solution was protected from room light by aluminum foil. The solution turned from deep blue to orange brown. The mixture was stirred for 2 h. Solvent was then removed by vacuum. The workup procedure from this point on was carried out in air but in the dark due to the light sensitivity of these compounds. The residue was triturated with ~300 mL of benzene or toluene and passed through a short column of silica gel or activated alumina. The filtrate was then rotary evaporated to dryness to give a brownish solid which was then redissolved in THF and passed through a short column of silica gel to give an orange-red filtrate. The addition of isooctane followed by slow evaporation of the solvent gave ca. 0.7 g of orange crystalline solid (typical yield <50%).

A few of the complexes were analyzed by Alfred Bernhardt, West Germany. Anal. Calcd for $Ph_3SnRe(CO)_3(phen)$: C, 49.52; H, 2.90; N, 3.50. Found: C, 49.34; H, 2.92; N, 3.26. Calcd for $Ph_3GeRe(CO)_3(phen)$: C, 52.54; H, 3.07; N, 3.71. Found: C, 52.66; H, 3.12; N, 3.84. Calcd for $Me_3SnRe(CO)_3(phen)$: C, 35.20; H, 2.79; N, 4.56. Found: C, 35.07; H, 2.76; N, 4.73. Calcd. for $Ph_3SnRe(CO)_3(biquin)$: C, 53.44; H, 3.10; N, 3.20. Found: C, 53.40; H, 3.12; N, 3.26. Calcd. for $Ph_3SnMn(CO)_3(phen)$: C, 59.23; H, 3.46; N, 4.19. Found: C, 59.01; H, 3.53; N, 4.00.

Synthesis of $R_3EM(CO)_5$ (R = Ph, Me; E = Sn; M = Mn, Re). The procedure used followed the literature method.[4,5] A typical synthetic procedure is as follows. A 4 mL sample of 1% Na/Hg was added to 1

(21) King, R. B. *Organomet. Synth.* **1965**, *1*, 174.
(22) Drew, D.; Darensbourg, D. J.; Darensbourg, M. Y. *Inorg. Chem.* **1975**, *14*, 1580.
(23) (a) Wong, C. L.; Kochi, J. K. *J. Am. Chem. Soc.* **1979**, *101*, 5593. (b) Hendrickson, D. N.; Sohn, Y. S.; Gray, H. B. *Inorg. Chem.* **1971**, *10*, 1559.

g of $Re_2(CO)_{10}$ (1.53×10^{-3} mol) dissolved in 15 mL of THF under Ar. The clear solution immediately turned from pale yellow to orange. After 2 h, excess of Na/Hg was removed, followed by the addition of 0.95 g of Ph_3SnCl (2.5×10^{-3} mol) in 25 mL of THF. The solution was then stirred for 2 days. A pale yellowish solution together with a white precipitate were observed. Removal of solvent and trituration with toluene gave a yellow solution that was then rotary evaporated to dryness. Recrystallization from ether and isooctane gave the white, crystalline solid $Ph_3SnRe(CO)_5$.

Synthesis of $[(CH_3CN)Re(CO)_3L]^+$ (L = phen, bpy, biquin). The synthetic procedure is similar to that reported in the literature.[24] A 0.4 g (1.55×10^{-3} mol) sample of $AgOSO_2CF_3$ was added to a suspension of 0.5 g (9.4×10^{-4} mol) of $BrRe(CO)_3(phen)$ in acetonitrile. The solution was then brought to reflux with stirring in the dark for 1 h. The precipitated AgBr was then filtered off to give a yellow filtrate which was then rotary evaporated to dryness. A brownish oil sometimes resulted. After several washings with ether, the residue was redissolved in a small amount of acetonitrile; upon addition of ether, 0.54 g of $[(CH_3CN)Re(CO)_3(phen)]OSO_2CF_3^-$ precipitated to give a yield of ca. 90%. Purity was confirmed by IR spectroscopy in the CO stretching region.

Emission Quantum Yields. The emission spectra were computer-corrected for the spectral sensitivity of the detection unit which in turn was calibrated by a 200-W tungsten–halogen standard lamp obtained from and calibrated by EGG, Inc., Salem, MA. The emission quantum yield of the Re complexes at 298 and 77 K in EPA were determined relative to rhodamine B in EtOH at 298 K ($\Phi = 0.69$).[25] When the absorbance at the chosen excitation wavelength is adjusted to be the same for the Re complex and that of rhodamine B in EtOH, the ratio of the area under the corrected emission spectra obtained for the Re complex and rhodamine B in EtOH, after corrections for the difference in the refractive index of the solvents multiplied by the emission quantum yield of rhodamine B, yields the emission quantum yield of the Re complex. The 298 K measurements were performed in a quartz cell with attachment for freeze–pump–thaw degassed 4 cycles and then sealed by a high vacuum Teflon stopcock. The excitation wavelength for emission quantum yields was a point where the absorption at 298 and 77 K are equal. Such an isoabsorbance point ensures that absorbance matching at 298 K remains valid for 77 K measurements. Note that 298 K emission yields are insensitive to excitation wavelength, while 77 K measurements may be modestly affected by variant in excitation wavelength (see Table V).

Emission Quenching Measurements. Solutions of constant concentration of $Ph_3SnRe(CO)_3(phen)$ (ca. 1×10^{-3} M) and variable concentration of quencher were prepared in CH_3CN containing 0.1 M of $[n\text{-}Bu_4N]PF_6$ and were freeze–pump–thaw degassed 4 cycles in 13×100 mm test tube, and hermetically sealed. To avoid the complication of unwanted emission from $(CH_3CN)Re(CO)_3(phen)^+$ (the net product generated by irradiating $Ph_3SnRe(CO)_3(phen)$ and an electron acceptor) and to achieve consistency, we monitored the emission intensity at 700 nm, 20-nm band-pass (red end of the emission band maximum) by briefly irradiating the sample with excitation wavelength between 500 and 510 nm, 2-nm band-pass (red end of the first absorption band). Linear Stern–Volmer plots[26] were obtained in all cases with at least 4 data points. The quenching rate constant, k_q, was obtained by dividing the slope of the Stern–Volmer plot by the emission lifetime at zero quencher concentration in the same solvent, electrolyte system, $\tau = 1.5 \times 10^{-6}$ s.

Electrochemical Measurements. Cyclic voltammetry and controlled potential electrolyses were carried out by using a PAR 173 potentiostat in conjunction with a 175 Universal Programmer and a 179 Digital Coulometer. The electrochemical cell was a three-electrode two-compartment cell system. The auxiliary electrode was a Pt foil separated by a fine-fritted disk from the main compartment containing the working electrode and the reference electrode. The working electrode was either a Pt bead electrode modified from a Polarographic Heyrovsky electrode (Sargent Welch) or a small piece of Pt wire (0.016 in. in diameter) sealed through glass with direct electrical contact to a copper wire. The reference electrode was either a commercial saturated calomel electrode (SCE) (Fischer) or a laboratory SCE constructed according to the literature method[27] with an Agar/KCl bridge immersed in a third compartment separated from the working electrode by a fine-fritted disk. During electrolysis, the coulombs passed were either measured by the 179 digital coulometer or manually integrated by using a recorded current–time plot.

The electrolytic reaction was analyzed by occasionally withdrawing a sample for either IR measurement to monitor the appearance of product or UV–vis measurement to monitor disappearance of reactant.

Chemical Oxidation of $R_3ERe(CO)_3(phen)$ and $(CO)_5ReRe(CO)_3(phen)$. Typically, the reaction was carried out in a Schlenk flask capped with a septum stopper under Ar. For example, a solution of 20 mL of CH_3CN containing 0.10 g of $Ph_3GeRe(CO)_3(phen)$ was vigorously stirred in the dark. Ceric ammonium nitrate was added in several fractions over a period of ca. 0.5 h. The solution was analyzed by IR, 5 min after each addition. IR analysis showed $[(CH_3CN)Re(CO)_3(phen)]^+$ to be formed quantitatively and required one equivalent of Ce^{4+}. For the $Ph_3SnRe(CO)_3(phen)$ quantitative formation of $[(CH_3CN)Re(CO)_3(phen)]^+$ requires 2 equiv of Ce^{4+} but only 1 equiv when $[Fe(\eta^5\text{-}C_5H_5)_2]^+$ is used as the oxidant. $(OC)_5ReRe(CO)_3(phen)$ was oxidized in CH_3CN solution by Ce^{4+} and by $Fe(phen)_3^{3+}$. The only products detected by IR were $[Re(CO)_5(CH_3CN)]^+$ and $[(CH_3CN)Re(CO)_3(phen)]^+$ requiring 2 equiv of the oxidant per $(OC)_5ReRe(CO)_3(phen)$.

Photolytic Quantum Yield Measurements. Samples of the Re complex ($(1\text{–}1.5) \times 10^{-3}$ M) were dissolved in CH_3CN solution containing 0.1 M of either $[n\text{-}Bu_4N]ClO_4$ or $[n\text{-}Bu_4N]PF_6$ and 2×10^{-3} to 6×10^{-2} M quencher. The solution was freeze–pump–thaw degassed 4 cycles in a 13-mm diameter test tube with a side arm for attachment to a quartz cell (1.0, 0.1, or 0.01 cm) and then sealed via a high-vacuum Teflon stopcock. The sample could then be irradiated through the test tube, and reaction in the case of quencher = PQ^{2+} could be monitored spectroscopically in the visible to follow the appearance of $PQ^{+\cdot}$ ($\lambda_{max} = 604$ nm; $\epsilon = 10060$ M^{-1} cm^{-1}).[28] IR spectra in the CO stretching region were used to monitor the reaction of the M complexes.

An Ar ion laser was used as the light source. Laser intensity was attenuated by Corning color glass filters and monitored by a calibrated beam splitter and a Tektronix J16 radiometer equipped with a J6502 probe.

Flash Photolysis. The flash photolysis measurement was carried out on a System 710 flash apparatus (Xenon Corporation). Typically, a CH_3CN solution containing $\sim 2 \times 10^{-4}$ M of $Ph_3GeRe(CO)_3(phen)$, $\sim 5 \times 10^{-3}$ M of TMPD or PQ^{2+}, and 0.1 M of $[n\text{-}Bu_4N]ClO_4$ was freeze–pump–thaw degassed for 4 cycles via a bulb attached to a cylindrical Pyrex cell into which the solution can then be transferred for flash photolytic measurements. The cell is 10 cm long in the analyzing beam path and 1 cm wide in the flash path. Experiments were also done by using a cylindrical cell provided with an outer jacket for the use of appropriate filter solution to filter out unwanted portions of the spectrum from the flash tube. A typical flash was ~ 300 J in energy and ~ 20 μs in duration. A He–Ne laser (632.8 nm) was used as the analyzing beam source. The transient absorption signals were detected by a RCA 1P21 photomultiplier tube powered by a Kepco Model ABS 1500 power supply and recorded on a Tektronix 564B storage oscilloscope and then photographed for permanent record.

Acknowledgment. We thank the National Science Foundation for support of this research. M.S.W. acknowledges support as a Dreyfus Teacher-Scholar grant recipient, 1975–1980.

(24) Edwards, D. A.; Marshalsea, J. *J. Organomet. Chem.* **1977**, *113*, 73.
(25) Calvert, J. G.; Pitts, J. N., Jr. "Photochemistry"; Wiley: New York, 1966.
(26) Turro, N. J. "Modern Molecular Photochemistry"; The Benjamin/Cummings Publishing Co., Inc.: 1978.
(27) Meites, L. "Polarographic Technique", 2nd ed.; Interscience: New York, 1963, p 63.
(28) Kosower, E. M.; Cotter, E. M. *J. Am. Chem. Soc.* **1964**, *86*, 5524.